ICSV 21
13-17 July, 2014, Beijing/China

The 21st International Congress on Sound and Vibration

13-17 July, 2014, Beijing/China

# ANALYTICAL STUDY OF A RIJKE TUBE WITH HEAT EXCHANGER

Aswathy Surendran, Maria A. Heckl

*Department of Computing and Mathematics, Keele University, Staffordshire, UK ST5 5BG, e-mail: a.surendran@keele.ac.uk*

Combustion systems are often integrated with heat exchangers to increase their efficiency and prolonged use. The thermo-acoustic instabilities in combustion systems had been the subject of research for over two decades. These instabilities occur due to the existence of feedback between the unsteady heat release rate and acoustic oscillations. The aim of this paper is to study how a tube row simulating a heat exchanger affects the stability behaviour. The setup is modelled as a Rijke tube. The upstream end is open and the downstream end is a row of tubes backed by a cavity. The speed of sound is assumed to be constant throughout the duct. The reflection coefficient of the downstream end of the duct depends on the cavity length, tube row properties and the resonant frequency of the system. The resonant frequency of the system is evaluated from the characteristic equation, developed from the boundary conditions at the tube ends and the heat source. The acoustic waves are assumed to be one-dimensional, with the heat source obeying the $n$-$\tau$ model for heat release rate. The parameters of interest in this study are: cavity length ($l_c$) and the radius of the heat exchanger tubes ($a$). Stability maps involving the growth rate of the acoustic oscillations in the system show the unstable/stable behaviour of the combustion system.

## 1. Introduction

Heat exchangers are widely used in internal combustion engines, refrigeration and air conditioning units, power plants etc., for effectively cooling the systems. These exchangers could be rows of cylindrical shells with a coolant fluid circulating through them. Hence, they bring about a periodicity in the structure and may exhibit resonance when acoustic waves are incident on them.

Combustion systems are often marred by the presence of thermo-acoustic instabilities. These instabilities occur as a result of the positive feedback existing between the unsteady heat release rate and acoustic pressure oscillations. Presently, the combustion system is modelled as a Rijke tube, which has inherent self-sustained and self-excited thermo-acoustic oscillations. The aim of this paper is to study the influence of a single tube row (heat exchanger) on the stability of the Rijke tube.

Previous studies have shown that tube bundles/banks scatter sound and in some cases may even absorb sound[1–4], depending on the tube row properties as well as the frequency of the incident wave. Howe[5] and Hughes and Dowling[6;7] have shown that perforated plates backed by a cavity, when placed at the inlet of a duct, effectively absorbed acoustic oscillations, thereby making the system stable. This was experimentally verified by Tran et. al.[8]. Stability predictions and analysis of Tran's combustor were carried out by Heckl and Kosztin[9]. Heckl[10] has experimentally shown that introduction of a feedback system in a Rijke tube can actively control the noise from the tube. The crux was to change

the reflection coefficient at the downstream end of the tube. An approach similar to Heckl's is adopted in the present study. The authors have tried to study the stability of the Rijke tube by introducing a tube row backed by cavity at the downstream end. It is expected that this arrangement will change the reflection coefficient of the downstream end.

## 2. Model of the combustion chamber with heat exchanger

The combustion chamber is modelled as a Rijke tube. The heat exchanger is simulated using a row of thin walled tubes, backed by a tuneable cavity, as shown in Fig. 1. The upstream end is at $x = 0$, and the downstream end is at $x = L$. The tube row, backed by the cavity, is located at the downstream end, and the heat source is located at a distance $l_h$ from the upstream end of the duct. The length of the cavity is denoted by $l_c$. The acoustic waves are assumed to be one–dimensional and the speed of sound inside the duct is considered to be uniform. The tube row is perpendicular to the wall of the Rijke tube.

### 2.1 Tube row

The individual tubes constituting the tube row are assumed to be thin-walled and follow the equations of motion given in section 7.12 of Junger and Feit[11]. The tubes have radius $a$ and thickness $h$. They are surrounded by an "outer" fluid and are filled with an "inner" fluid which are denoted by the subscripts '$o$' and '$i$' respectively. A one-dimensional array of such tubes, spaced by distance $d$, forms the tube row which simulates the heat exchanger (Fig. 2). We have followed the work of Huang and Heckl[3] to obtain the reflection and transmission coefficients of the tube row. They have applied the theory of diffraction grating, initially proposed and described by Twersky[12], to obtain these coefficients. The reader is advised to refer to their work for details, as we have provided only the final expressions for the reflection and transmission coefficients derived by them. The transmission and reflection coefficients for a single tube row are:

$$T_t = 1 + \frac{2}{k_o d}\,\frac{1}{cos\phi_o}\,\sum_{n=-\infty}^{\infty} A_n\, e^{in\phi_o} \tag{1}$$

$$R_t = \frac{2}{k_o d}\,\frac{1}{cos\phi_o}\,\sum_{n=-\infty}^{\infty} A_n\, e^{in(\pi-\phi_o)} \tag{2}$$

where $k_o$ is the wavenumber in the outer fluid, $A_n = a_n\left(e^{-in\phi_o} + \sum_{m=-\infty}^{\infty} A_m\, F_{n-m}\right)$ and $F_{n-m}$ is the Schlömilch series which depends on the angle of incidence $\phi_o$, tube spacing $d$ and wavelength in the outer fluid $\lambda_o$. $a_n$ is the scattering coefficient of an individual tube within the tube row.

Figs. 3 and 4 show the transmission and reflection coefficients of a tube row, calculated using Eq. (1) and Eq. (2), for $\phi_o = 0$ and two different values of the tube radius $a$: 0.01m and 0.015m.

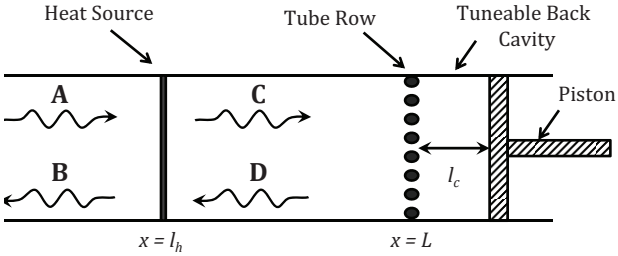


**Figure 1**: Schematic of the combustion chamber with heat exchanger.

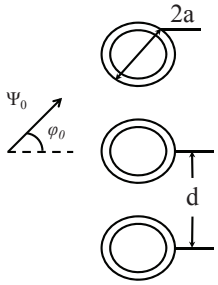


**Figure 2**: Geometry of the tube row.

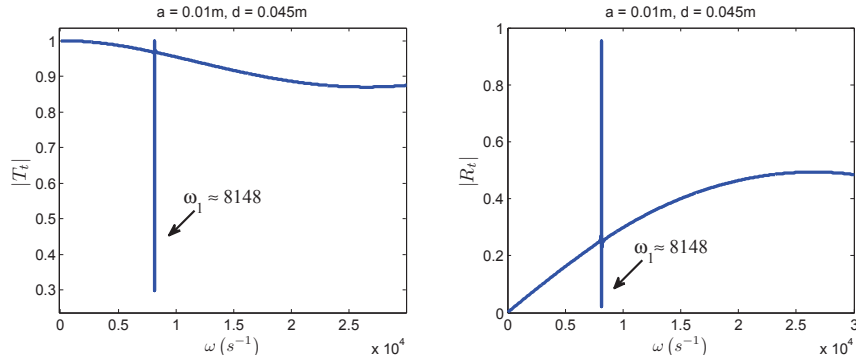


**Figure 3**: $|T_t|$ and $|R_t|$ for a tube row with $a$ = 0.01m, $d$ = 0.045m and $h$ = 0.001m.

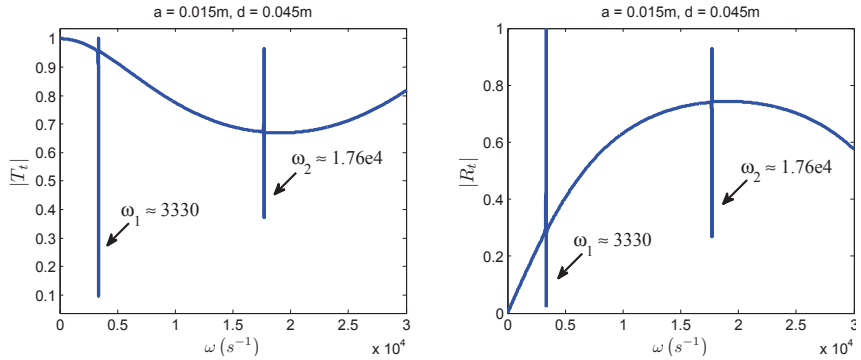


**Figure 4**: $|T_t|$ and $|R_t|$ for a tube row with $a$ = 0.015m, $d$ = 0.045m and $h$ = 0.001m.

The peaks in Figs. 3 and 4 are due to resonance of the individual tubes. We observe that the resonance frequencies are higher for radius $a$ = 0.01m than for $a$ = 0.015m. This is plausible because, given that the wall thickness and tube spacing are the same in the two figures, the tube with the larger radius is "softer".

## 2.2 Tube row backed by cavity

In this section, we derive the "combined reflection coefficient", i.e., the reflection coefficient of the tube row backed by a cavity, as shown in Fig. 5. The tube row is located at $x = 0$ with the moveable piston at $x = l_c$. The transmission ($T_t$) and reflection ($R_t$) coefficients of the tube row are given by Eq. (1) and Eq. (2) respectively, and $R_p$ is the reflection coefficient at the downstream end of the cavity. The pressure and velocity field for the given configuration is obtained by superposing the travelling waves upstream and downstream of the tube row.

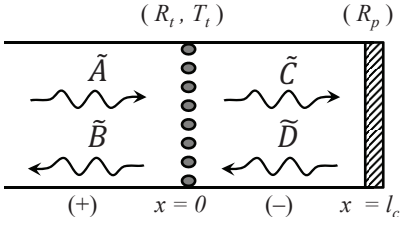


**Figure 5**: Schematic of tube row with cavity

$$\tilde{p}(x) = \begin{Bmatrix} \tilde{A}e^{ikx} + \tilde{B}e^{-ikx} & x < 0 \\ \tilde{C}e^{ikx} + \tilde{D}e^{-ikx} & l_c < x < 0 \end{Bmatrix} \tag{3}$$

$$\tilde{u}(x) = \frac{1}{\rho_o c_o} \begin{Bmatrix} \tilde{A}e^{ikx} - \tilde{B}e^{-ikx} & x < 0 \\ \tilde{C}e^{ikx} - \tilde{D}e^{-ikx} & l_c < x < 0 \end{Bmatrix} \tag{4}$$

where $\rho_o$ is the density and $c_o$ is the speed of sound in the outer fluid. The factor of $e^{-i\omega t}$ is omitted in the present analysis. $\tilde{A}$, $\tilde{B}$, $\tilde{C}$ and $\tilde{D}$ are the complex pressure amplitudes upstream and downstream of the tube row. They have to be such that the following boundary conditions are satisfied:

$$At\ x = 0: \quad \begin{cases} \tilde{C} = T_t\tilde{A} + R_t\tilde{D} \\ \tilde{B} = T_t\tilde{D} + R_t\tilde{A} \end{cases} \tag{5}$$

$$At\ x = l_c: \quad \tilde{D}e^{-ikl_c} = R_p\tilde{C}e^{ikl_c} \tag{6}$$

The combined reflection coefficient is given by the amplitude ratio $\tilde{B}/\tilde{A}$ and this can be obtained from Eq. (5) and Eq. (6). The result is:

$$R_{comb} = \frac{\tilde{B}}{\tilde{A}} = R_t + \frac{R_p T_t^2 e^{2ikl_c}}{1 - R_p R_t e^{2ikl_c}}\,. \tag{7}$$

### 2.3 Heat release rate

The heat source is assumed to be a planar sheet that is confined to an infinitesimally thin region at $x = l_h$. The heat release rate follows the *n*–$\tau$ model, i.e., it depends on the velocity field existing at $l_h$ $((u(x = l_h))$, but after a time lag $\tau$.
In the time domain:

$$Q\,(x,t) = nu\,(x, t-\tau) \tag{8}$$

In the frequency domain:

$$Q\,(x,\Omega) = nu\,(x)\,e^{i\Omega\tau} \tag{9}$$

### 2.4 Rijke tube with heat exchanger

The Rijke tube is a straight duct with open ends, containing a heat source within. In the present study, the downstream end of the duct is fitted with a tube row backed by cavity. This is shown in Fig. 6. The pressure and velocity field for such a system is given by:

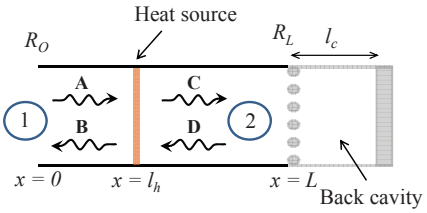


**Figure 6**: Schematic of the Rijke tube with heat exchanger.

Region 1:

$$p_1(x) = Ae^{ik(x-l_h)} + Be^{-ik(x-l_h)} \qquad 0 < x < l_h \tag{10}$$

$$u_1(x) = \frac{1}{\rho_o c_o}\left\{Ae^{ik(x-l_h)} - Be^{-ik(x-l_h)}\right\} \qquad 0 < x < l_h \tag{11}$$

Region 2:

$$p_2(x) = Ce^{ik(x-l_h)} + De^{-ik(x-l_h)} \qquad l_h < x < L \tag{12}$$

$$u_2(x) = \frac{1}{\rho_o c_o}\left\{Ce^{ik(x-l_h)} - De^{-ik(x-l_h)}\right\} \qquad l_h < x < L \tag{13}$$

*A*, *B*, *C* and *D* are pressure amplitudes that are to be determined.
The heat release rate can be expressed with Eq. (9) as:

$$Q'\,(x = l_h) = ne^{i\Omega\tau}\frac{(A-B)}{\rho_o c_o}\,. \tag{14}$$

We assume the following boundary conditions:
At $x = 0$:

$$Ae^{-ikl_h} = R_o B e^{ikl_h} \tag{15}$$

At $x = L$:

$$De^{-ik(L-l_h)} = R_L C e^{ik(L-l_h)} \tag{16}$$

At $x = l_h$, we assume continuity of pressure,

$$A + B = C + D \,, \tag{17}$$

and a velocity jump generated by the heat source

$$-(A - B) + (C - D) = \frac{(\gamma - 1)}{Sc_o} Q'(l_h) \,, \tag{18}$$

where $S$ is the area of cross section of the duct, $R_o$ (open end) and $R_L$ (given by Eq. (7)) are the reflection coefficients at $x$ = 0 and $x = L$ respectively, and $\gamma$ is the ratio of the specific heat capacities.

## 3. Methodology

The stability of the Rijke tube is determined using the eigenvalue method.

### 3.1 Calculation of complex eigenvalues

Eqs. (15)–(18) can be written as a set of homogeneous equations for the unknowns $A, B, C$ and $D$.

$$[Y(\Omega)] = \begin{bmatrix} A \\ B \\ C \\ D \end{bmatrix} = \begin{bmatrix} 0 \\ 0 \\ 0 \\ 0 \end{bmatrix} \,, \tag{19}$$

with

$$Y(\Omega) = \begin{bmatrix} e^{-i\frac{\Omega}{c_o}l_h} & -R_o e^{i\frac{\Omega}{c_o}l_h} & 0 & 0 \\ 0 & 0 & R_L e^{i\frac{\Omega}{c_o}(L-l_h)} & -e^{-i\frac{\Omega}{c_o}(L-l_h)} \\ 1 & 1 & -1 & -1 \\ -1-\beta e^{i\Omega\tau} & 1+\beta e^{i\Omega\tau} & 1 & -1 \end{bmatrix} \,, \tag{20}$$

where $\beta = (n(\gamma - 1)) / (S\rho_o c_o^2)$ .
The eigenvalues are the solutions of the characteristic equation

$$\det Y(\Omega) = 0 \,, \tag{21}$$

where

$$\begin{aligned} \det Y(\Omega) = &-2e^{-i\frac{\Omega}{c_o}L} + 2R_o R_L e^{i\frac{\Omega}{c_o}L} + \beta e^{i\Omega\tau}\Big(-e^{-i\frac{\Omega}{c_o}L} + R_o R_L e^{i\frac{\Omega}{c_o}L} + \\ &R_o e^{-i\frac{\Omega}{c_o}(L-2l_h)} - R_L e^{i\frac{\Omega}{c_o}(L-2l_h)}\Big) \,. \end{aligned} \tag{22}$$

### 3.2 Stability analysis

$\Omega$ is the complex eigenfrequency. It can be determined by solving Eq. (21) numerically, for example, by the Newton - Raphson technique. The results are of the form

$$\Omega_n = \omega_n + i\delta_n \,, \tag{23}$$

where $\omega_n$ is the natural frequency of the mode $n$ and $\delta_n$ is the growth rate. Positive $\delta_n$ indicates instability and negative $\delta_n$ indicates stability.

# 4. Results and Discussion

## 4.1 Numerical values for various parameters used

*Duct properties:*
$S =$ $0.01\ m^2$ (cross–sectional area of the duct)
$L =$ $0.3\ m$ (length of the duct)
*Heat source location* $l_h \epsilon\ [0, L]\ m$
*Cavity length* $l_c \epsilon\ [0, L/2]\ m$
*Tube row properties:*
$E =$ $2 \times 10^{11}\ N/m^2$ (Young's modulus of steel)
$\sigma =$ $0.3$ (Poisson ratio)
$c_w =$ $5000\ m/s$ (compressional wave speed on a steel plate)
$a =$ $0.01\ m$ and $0.015\ m$ (tube radius)
$h =$ $0.001\ m$ (tube thickness)
$d =$ $0.045\ m$ (tube spacing)

*Inner fluid properties:*
$c_i =$ $1460\ m/s$ (speed of sound in water)
$\rho_i =$ $1000\ kg/m^3$ (density of water)
$\gamma_i =$ $10$
*Outer fluid properties:*
$c_o =$ $358\ m/s$ (speed of sound in air)
$\rho_o =$ $1.21\ kg/m^3$ (density of air)
$\gamma_o =$ $1.4$
*Heat release rate model:*
$\tau =$ $0.15 \times 10^{-3} s$ (time - lag)
$n =$ $187\ kg\ m/s^2$
*Downstream end conditions:*
$R_p = 1$ (for termination by piston)
$R_p = -1$ (for open end)

## 4.2 Stability Maps

The stability analysis is conducted for two duct end conditions: open-open and open-closed. Stability maps were produced by calculating the growth rate $\delta_n$, for the first mode ($n$ = 1). Stable regions ($\delta_n < 0$) are indicated by light regions and unstable regions ($\delta_n > 0$) by dark regions, in the figures below. The parameters of interest are $l_c$ (cavity length) and $l_h$ (heat source location).

Fig. 7 shows stability maps for the case where the tube row is absent. The results show the expected behaviour of a Rijke tube: For open-open ends, the system is unstable when the heat source is in the upstream half, and stable when the heat source is in the downstream half of the tube (see Fig. 7(a)). The reduction of the stable region with increasing $l_c$ is due to the fact that the total length of the duct, $L + l_c$, increases. For the open-closed situation, the Rijke tube is always unstable (Fig. 7(b)).

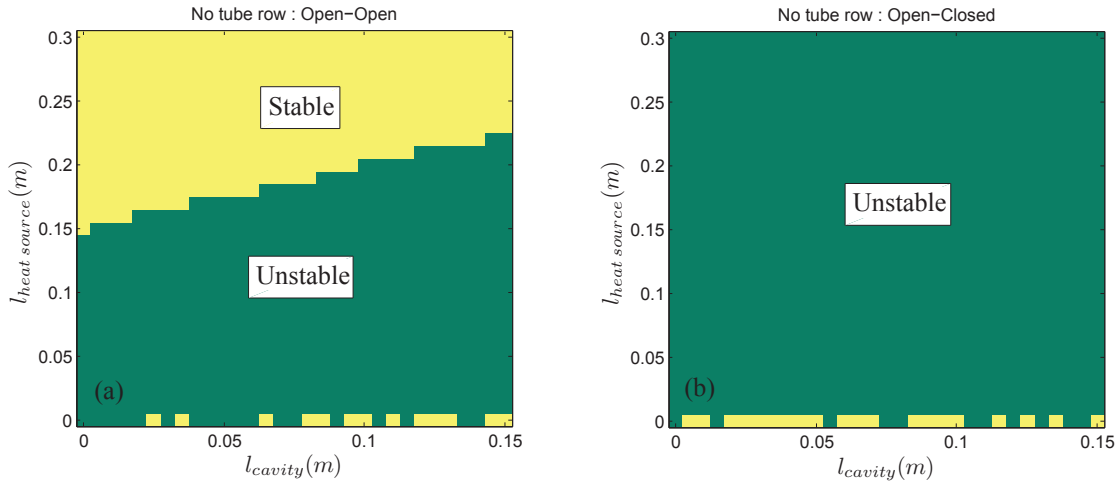


**Figure 7**: Stability maps for the duct with no tube row and (a) Open-open end condition (b) Open-closed end condition.

The range of frequencies is [2000 $s^{-1}$,4000 $s^{-1}$] for the open-open case, and [500 $s^{-1}$,2000 $s^{-1}$] for the open-closed case. This means that the period of the oscillation is of the order $10^{-3} s$, i.e., the time-lag $\tau$ is much less than that.

We now assume the tube row to be present and determine the stability maps for two values of the tube radius $a$, again for an open-open and open-closed duct. Fig. 8 shows the result for $a$ = 0.01m.

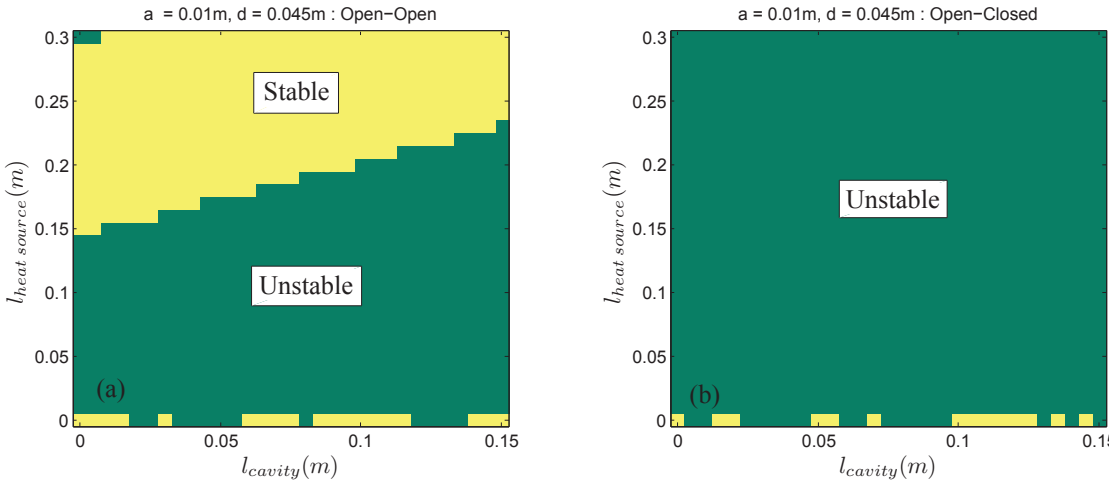


**Figure 8**: Stability map for $a$ = 0.01m, $d$ = 0.045m and $h$ = 0.001m for (a) Open-open end condition and (b) Open-closed end condition.

The stability maps are very similar to those for the "no tube row" case (see Fig. 7). Here, the range of frequencies is [2000 $s^{-1}$,4000 $s^{-1}$] for the open-open case, and [1000 $s^{-1}$,2000 $s^{-1}$] for the open-closed case.

For $a$ = 0.015m, the picture is quite different, as can be seen from Fig. 9. The frequency range is [2000 $s^{-1}$,4000 $s^{-1}$] for the open-open case, and [1500 $s^{-1}$,3500 $s^{-1}$] for the open-closed case.

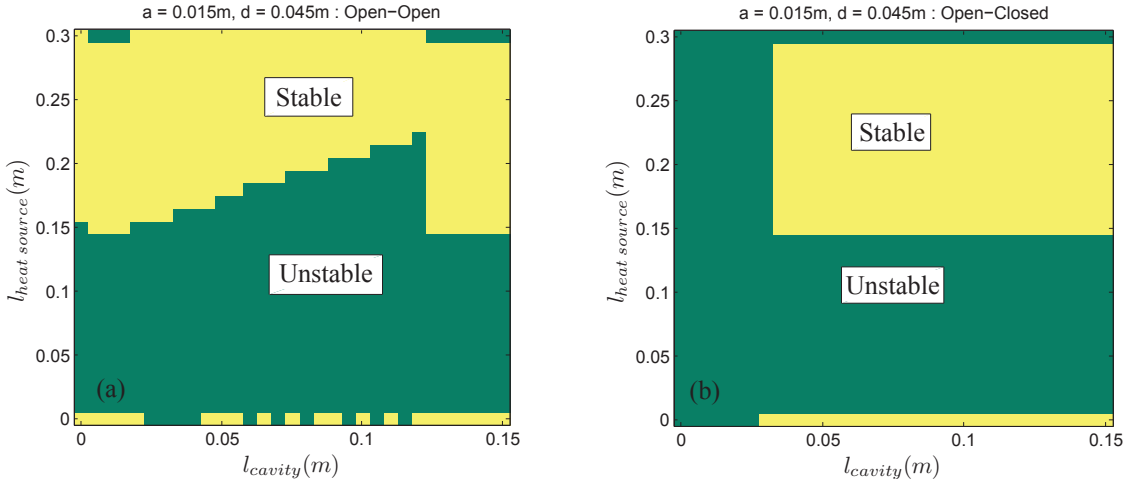


**Figure 9**: Stability map for $a$ = 0.01m, $d$ = 0.045m and $h$ = 0.001m for (a) Open-open end condition and (b) Open-closed end condition.

There is a marked change in the stability behaviour, both for the open-open and open-closed case. The reason for this lies in the resonant behaviour of the heat exchanger tubes. For the stiff tubes ($a$ = 0.01m), the first resonance occurs at $\omega_1 \approx 8148\ s^{-1}$ (Fig. 3), which is outside the frequency range covered by mode 1 in the Rijke tube. For softer tubes ($a$ = 0.015m), the first resonance is at $\omega_1 \approx 3330\ s^{-1}$(Fig. 4), and this clearly falls within the range of frequency values where the Rijke tube (with tube row present) exhibits resonance for the different values of $l_c$ and $l_h$. At the resonance frequency of the tube row, the reflection coefficient will be minimal and the wave incident on the tube row will be trapped within the cavity i.e.,diverted away from the heat source, thereby affecting the stability of the system.

## 5. Summary and Outlook

It was shown that introducing a tube row backed by cavity could alter the reflection coefficient at the duct boundaries. However, to have an effect on the stability behaviour of the duct, the duct resonating frequency and the tube row resonating frequency must match. In order to achieve this, the radius of the tube in the tube row is varied. This could also be brought about by varying the tube spacing or the thickness of the tube. Currently, work is being done in introducing dissipation methods and base flow within the tube row to closely resemble real-life situations.

## Acknowledgement

The presented work is part of the Marie Curie Initial Training Network Thermo-acoustic and aero-acoustic nonlinearities in green combustors with orifice structures (TANGO). We gratefully acknowledge the financial support from the European Commission under call FP7-PEOPLE-ITN-2012.

## References

[1] Blevins, R. D. and Bressler, M. M., Experiments on acoustic resonance in heat exchanger tube bundles, *Journal of Sound Vibration*, **164** (3), 503–533, (1993).

[2] Heckl, Maria A. and Mulholland, L. S., Some recent developments in the theory of acoustic transmission in tube bundles, *Journal of Sound and Vibration*, **179**(1), 37–62, (1995).

[3] Heckl, Maria A., Sound Propagation in Bundles of Periodically Arranged Cylindrical Tubes, *Acustica*, **77**(3), 143–152, (1992).

[4] Huang, X. Y. and Heckl, Maria A., Transmission and Dissipation of Sound Waves in Tube Bundles, *Acustica*, **78**(4), 191–200, (1993).

[5] Howe, M. S., *Acoustics of Fluid-Structure Interactions*, Cambridge University Press, Cambridge, UK, (1998).

[6] Hughes, I. J. and Dowling, A. P., The absorption of sound by perforated linings, *Journal of Fluid Mechanics*, **218**, 299–335, (1990).

[7] Dowling, A. P. and Hughes, I. J., Sound absorption by a screen with a regular array of slits, *Journal of Sound and Vibration*, **156**(3), 387–405, (1992).

[8] Tran, N., Ducruix, S. and Schuller, T., Damping combustion instabilities with perforates at the premixer inlet of a swirled burner, *Proceedings of the Combustion Institute*, **32**, 2917–2924, (2009).

[9] Heckl, Maria A. and Kosztin, B., Analysis and control of an unstable mode in a combustor with tuneable end condition, *International Journal of Spray and Combustion Dynamics*, **5**(3), 243–272, (2013).

[10] Heckl, Maria A., Active control of the noise from a Rijke tube, *Journal of Sound and Vibration*, **124**(1), 117–133, (1988).

[11] Junger, M. C. and Feit, D., *Sound Structures and Their Interaction*, The MIT Press, Cambridge, Massachusetts, (1986).

[12] Twersky, V., Elementary function representations of Schlömilch series, *Archive for Rational Mechanics and Analysis*, **8**(1), 323–332, (1961).